Supplement of Geosci. Model Dev., 17, 1443–1468, 2024
https://doi.org/10.5194/gmd-17-1443-2024-supplement

Geoscientific Model Development
Open Access
EGU

Supplement of

Benchmarking GOCART-2G in the Goddard Earth Observing System (GEOS)

Allison B. Collow et al.

Correspondence to: Allison B. Collow (allison.collow@nasa.gov)

S1. Technical Details for Updates in GOCART-2G

S1.1 Implementation of Primary Organic Aerosol

Beginning with GOCART-2G, a distinction is made between "weakly-absorbing" anthropogenic and "absorbing" (also referred to as "brown") biomass burning organic aerosol. Anthropogenic emissions of organic carbon, which are emitted based on CEDS, are solely considered to be "non-absorbing" organic carbon, with spectral optical properties that follow the OPAC database and are as in Chin et al. (2002) and Colarco et al. (2010). Biomass burning emissions of organic carbon from the Quick Fire Emissions Dataset (QFED) are considered absorbing "brown" carbon and assigned optical properties that have spectrally varying absorption at wavelengths shorter than 550 nm as described in Colarco et al. (2017). This distinction was found in Colarco et al. (2017) to improve the comparison of the absorbing aerosol-sensitive aerosol index between the model and data retrieved from the Ozone Monitoring Instrument (OMI) onboard the NASA Aura spacecraft. The optical properties between our absorbing and non-absorbing organic aerosol components are identical at wavelengths equal to and greater than 550 nm and treated by identical chemical and loss processes in the model.

S1.2 Implementation of Secondary Organic Aerosol

A simplified SOA mechanism is employed that scales VOC emissions in terms of carbon monoxide (CO) emissions from anthropogenic and biomass sources. Following Kim et al. (2015) we assume production of anthropogenic VOC at a rate of 0.069 g (g CO)$^{-1}$ and biomass burning VOC at a rate of 0.013 g (g CO)$^{-1}$. The VOC tracers are advected and assumed to convert to SOA via reaction with the prescribed MERRA-2 GMI OH fields with a rate constant of 1.25x10^{-11} cm^3 molecule^{-1} sec^{-1} (Hodzic and Jimenez, 2011). The SOA produced is apportioned to the hydrophilic modes of organic (anthropogenic) and brown (biomass burning) carbon. Biogenic VOCs, including isoprene, monoterpene, and other terpenes are provided from the Model of Emissions of Gases and Aerosols from Nature (MEGAN; Guenther et al., 2012) and enter the model through the Harvard–NASA Emission Component software (HEMCO, Keller et al., 2014) and are assigned to the hydrophilic mode of the organic carbon component. Unlike anthropogenic and biomass burning SOA that are produced in the air via the reaction of VOCs and OH, biogenic SOA is produced by scaling MEGAN emitted VOCs at the point of emission.

S1.3 Implementation of Stratospheric Sulphate Aerosol

An optional simplified stratospheric sulphate mechanism is implemented following the mechanism described in English et al. (2011). A tracer for carbonyl sulphide (OCS) is added to the model, with a prescribed surface mixing ratio boundary condition of 490 ppt$_v$, and is transported by the model such that chemistry can occur in the stratosphere OCS is largely inert in the troposphere and the model has been spun up so that a well-mixed distribution is achieved. Photochemical destruction of OCS is managed by the stratospheric chemistry package StratChem described in Nielsen et al. (2017). The reactions considered include binary consumption of OCS by OH and atomic oxygen, O(^{3}P), and photolytic destruction of OCS (the dominant process), using rate constants from Sander et al. (2011). The sulphur is assumed oxidized to SO_2 and then passed to GOCART, which computes the sulphate aerosol production using the same series of reactions as above for the tropospheric sulphate aerosol production. This mechanism provides us a simplified representation of the naturally occurring background stratospheric sulphate. While this mechanism is included in the benchmark experiment analysed in Section 4, it is currently not intended for use in an operational system like GEOS FP as it is computationally expensive.

S1.4 Code Refactoring

GOCART has been split into its own repository (https://github.com/GEOS-ESM/GOCART.git) with specific low-level interfaces that do not depend on the Earth System Model Framework (ESMF, https://earthsystemmodeling.org) and are independent of the overall GEOS architecture. This allows for code to be effectively shared with external organizations. Performance was enhanced through optimization of settling and nitrate chemistry parameterizations, eliminating extraneous calculations, and removing known bugs. The other code refactoring consisted of eliminating non-standard Fortran, eliminating redundant and legacy constructs, reducing duplicated logic within and across components, implementing cleaner component resource files, improving procedure and variable names in the source code to make the intent obvious to users and developers, and splitting large procedures with well-defined responsibilities.

A large component of the refactoring involved more widespread adoption of the ESMF within the parent GOCART-2G component. Improved flexibility within the code is essential for future development of GOCART-2G within GEOS. Carbon, sulphate, nitrate, sea salt, and dust, now have their own ESMF components and can instantiate multiple active and/or passive instances at one time; an active instance participates in the physical coupling with the host model. For example, carbonaceous aerosol is one of GOCART-2G's children and black, brown, and organic carbon are each run as an active instance of the carbonaceous aerosol component. This means that the model is provided with characteristics of each carbon species, including optics, density, particle radius, and the fraction that enters as hydrophobic, and black, brown, and organic carbon utilize the same code to perform process-related calculations, thus eliminating duplicated code. An example of a passive instance that could be run using the same methodology would be to track and provide diagnostics for the portion of a species from a specific emission source, such as sulphate formed from in response to volcanic emissions.

S2. Supplemental Figures

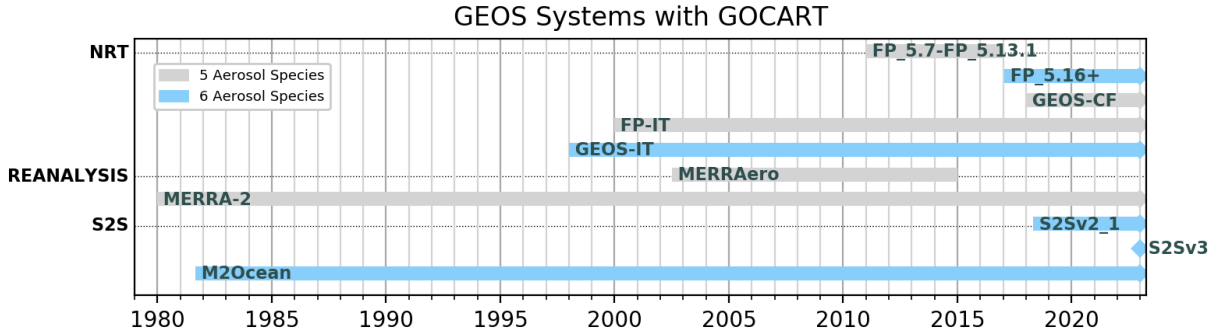

Figure S1: Timeseries of available data from operational GEOS systems coloured based on the configuration of GOCART

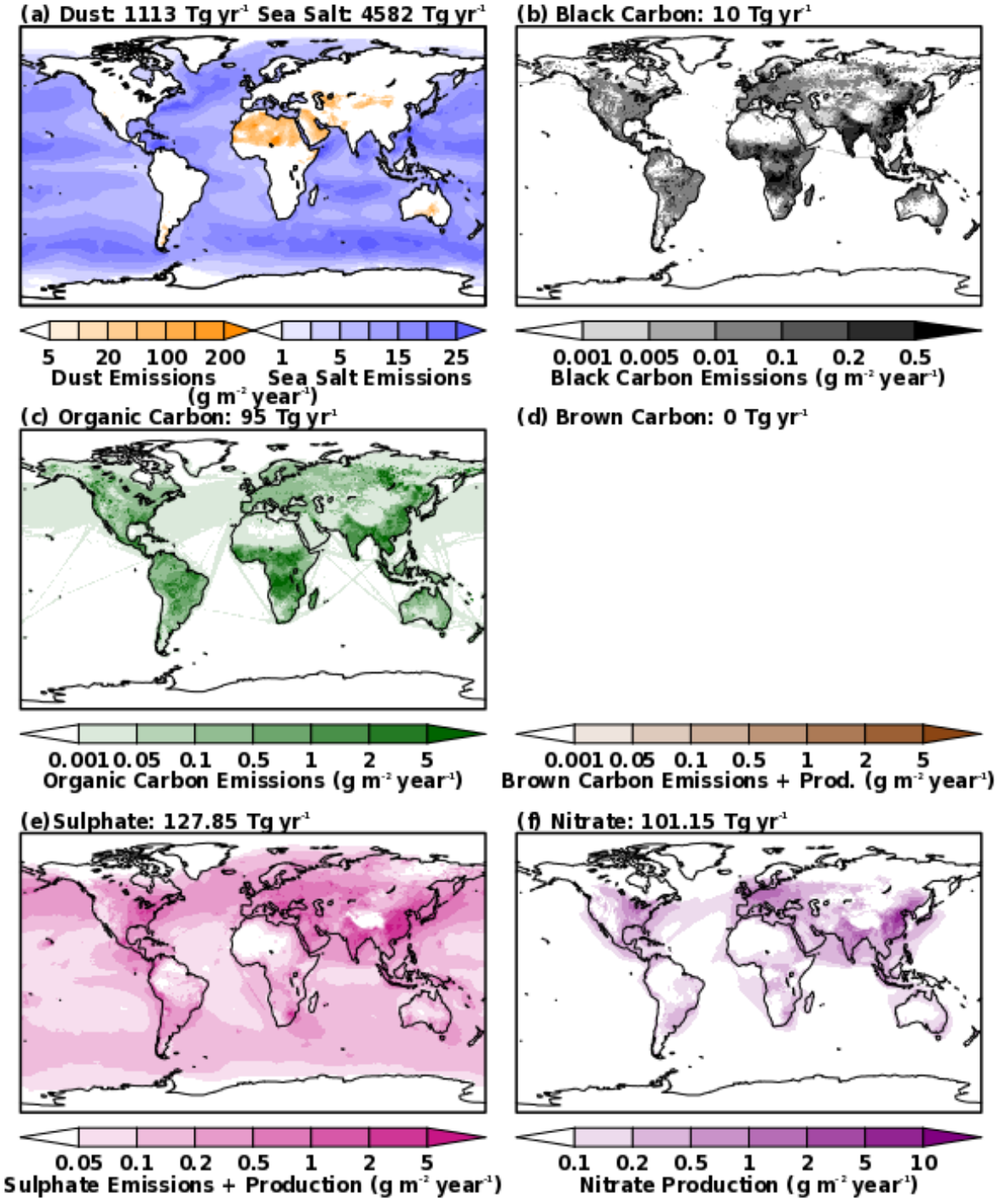

Figure S2: Emissions of (a) dust, sea salt, (b) black carbon, (c) organic carbon, (d) brown carbon, and (e) sulphate as well as the production of (d) brown carbon from secondary organic aerosol, (e) sulphate, and (f) nitrate averaged for the period of January 2016 through December 2016 in the GEOS Legacy GOCART simulation.

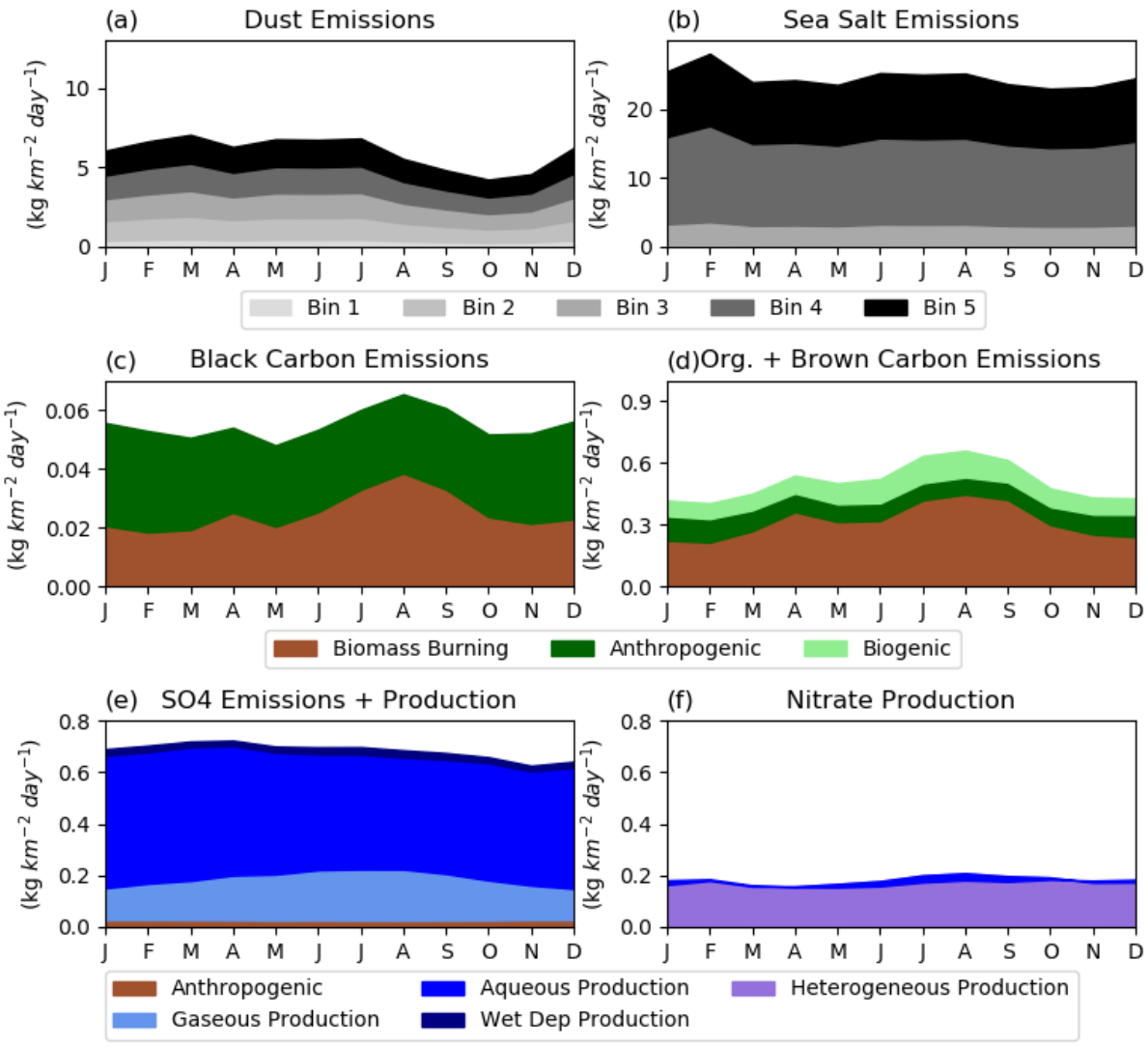

Figure S3: Timeseries of emissions and production of (a) dust, (b) sea salt, (c) black carbon, (d) organic carbon, (e) sulphate, and (f) nitrate for the period of January 2016 through December 2016 in the GEOS Legacy GOCART simulation.

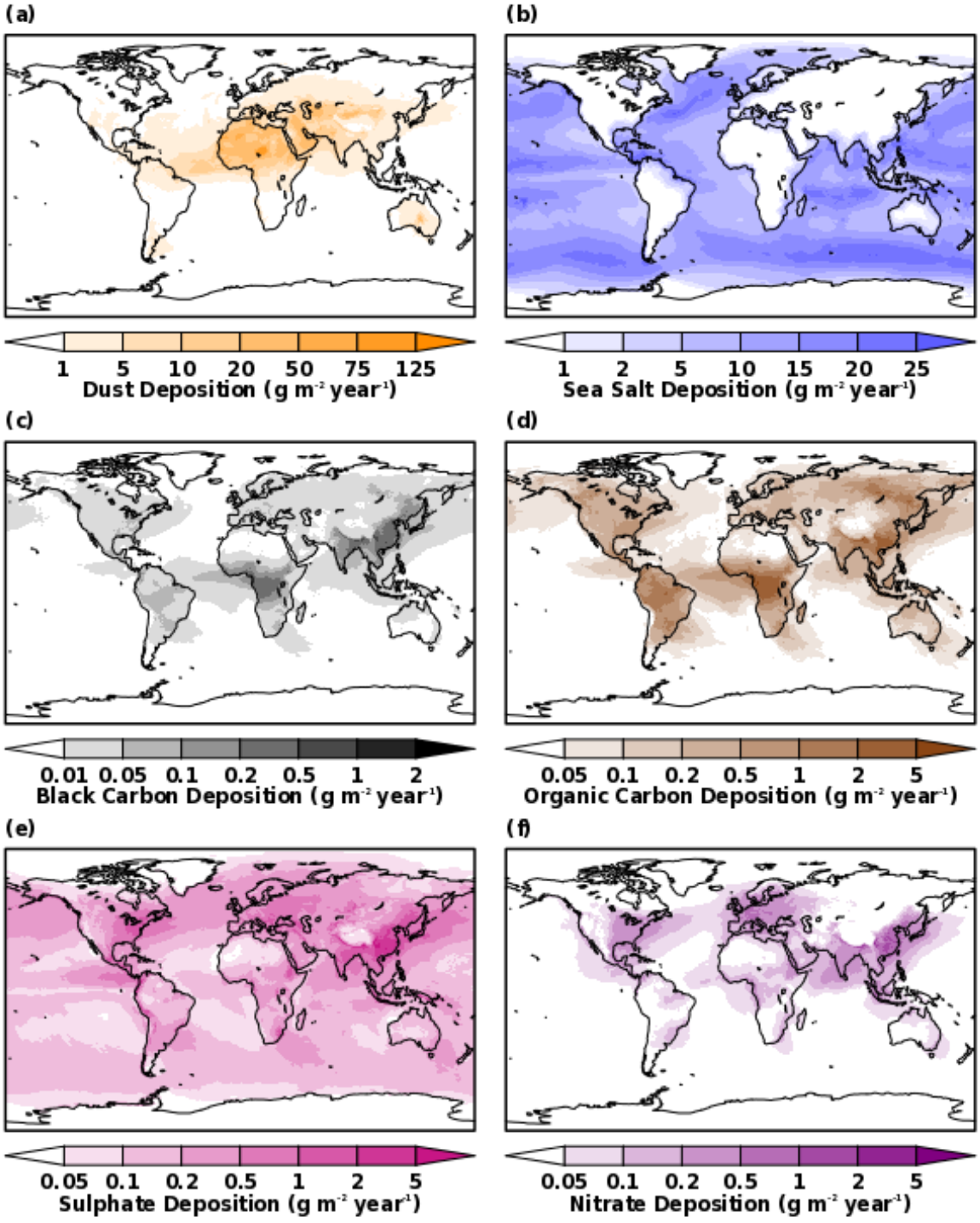

Figure S4: Deposition of (a) dust, sea salt, (b) black carbon, (c) organic carbon, (d) brown carbon, (e) sulphate, and (f) nitrate averaged for the period of January 2016 through December 2016 in the GEOS Legacy GOCART simulation.

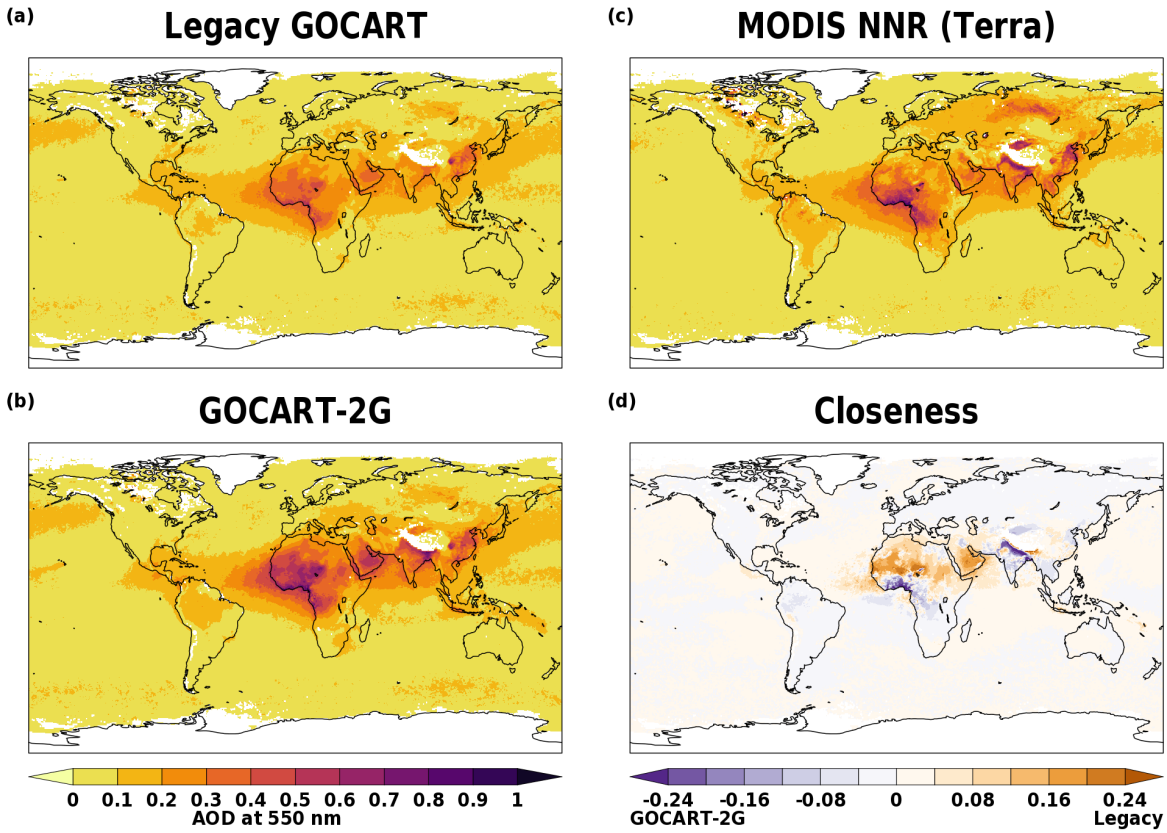

Figure S5: Average AOD at 550 for the period of January 2016 through December 2016 in the (a) GEOS Legacy GOCART simulation, (b) GEOS GOCART-2G benchmark simulation, (c) MODIS NNR observational product from Terra, and (d) the closeness to the observations defined as |GOCART-2G-MODIS| - |Legacy GOCART -MODIS|.

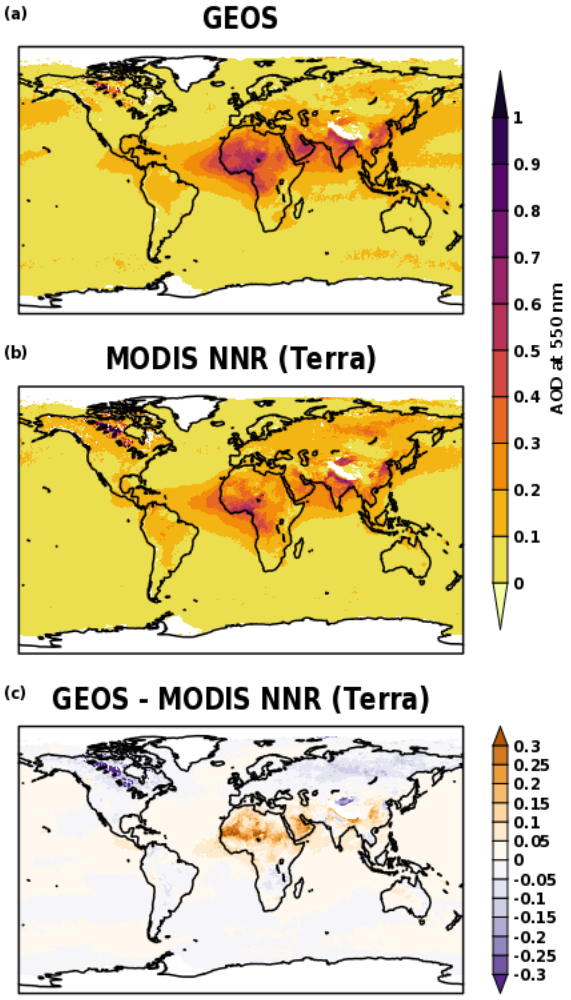

Figure S6: Average AOD at 550 for the period of January 2016 through December 2019 in the (a) GEOS GOCART2G benchmark simulation, (b) MODIS NNR observational product from Terra, and (c) the difference between the model and observations.

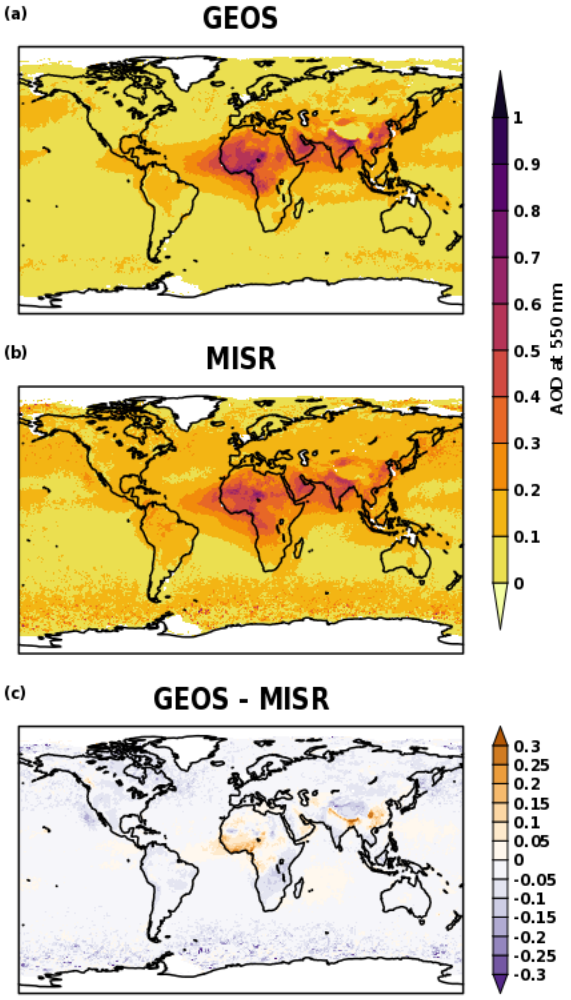

Figure S7: Average AOD at 550 for the period of January 2016 through December 2019 in the (a) GEOS GOCART2G benchmark simulation, (b) MISR, and (c) the difference between the model and observations.

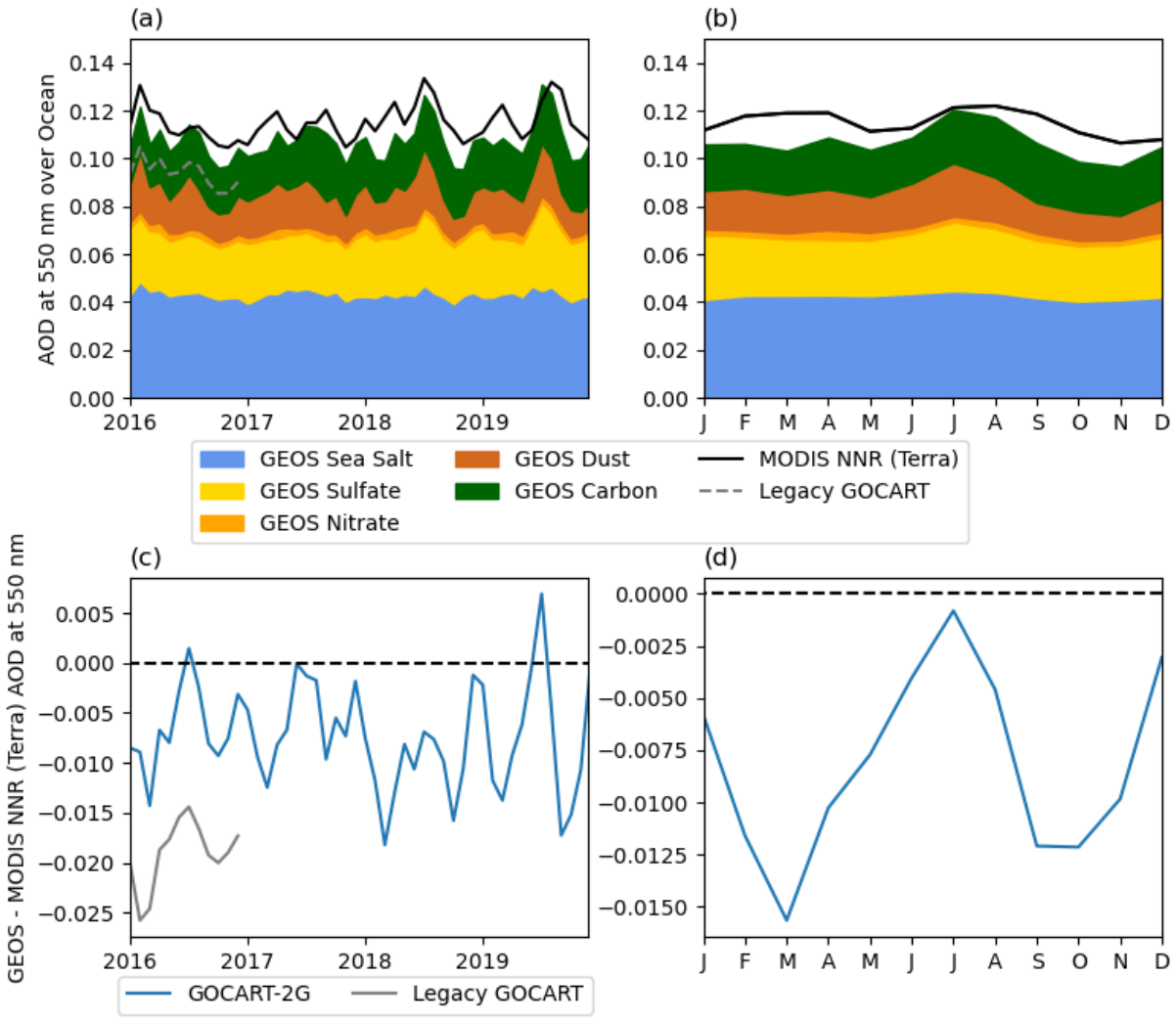

Figure S8: Timeseries of ocean area-averaged (a) monthly mean AOD from the Terra MODIS NNR observational product and the speciated AOD from the GEOS GOCART2G benchmark simulation, (b) mean seasonal cycle, and the difference between the model and observations for the (c) monthly mean AOD and (d) seasonal cycle of AOD. Gray lines are added in (a) and (c) for legacy GOCART during 2016 for reference.

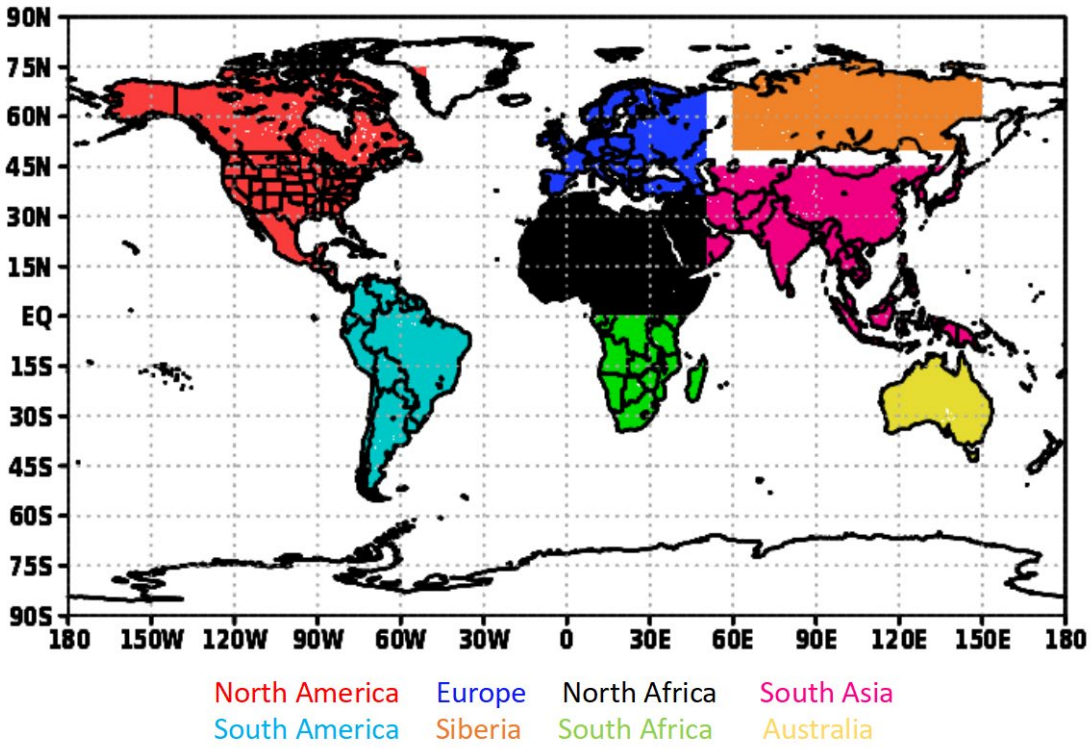

Figure S9: Map showing the area averaged regions for the AOD timeseries.

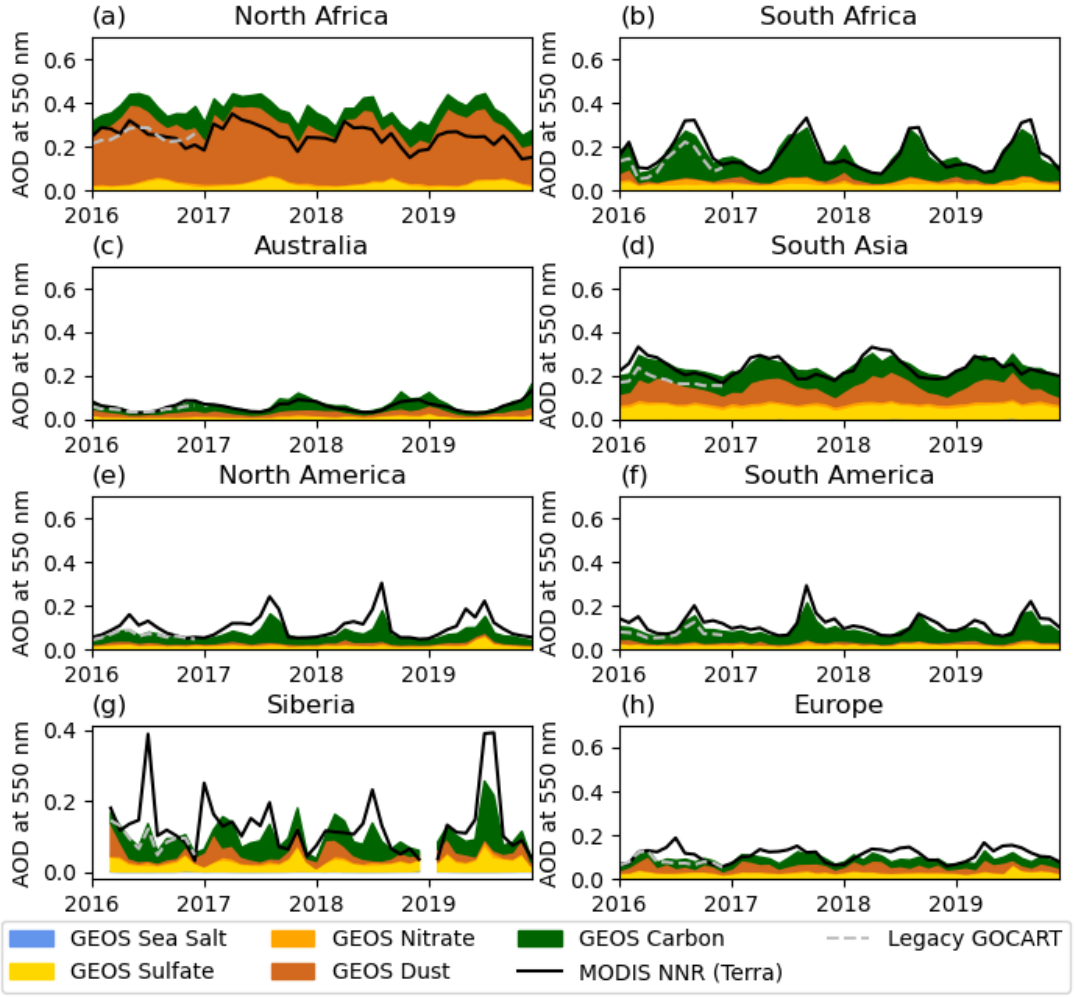

Figure S10: Timeseries of area-averaged monthly mean AOD from the Terra MODIS NNR observational product and the speciated AOD from the GEOS GOCART2G benchmark simulation over (a) North Africa, (b) South Africa, (c) Australia, (d) South Asia, (e) North America, (f) South America, (g) Siberia, and (h) Europe. Gray lines are added for the legacy GOCART simulation in 2016 for reference.

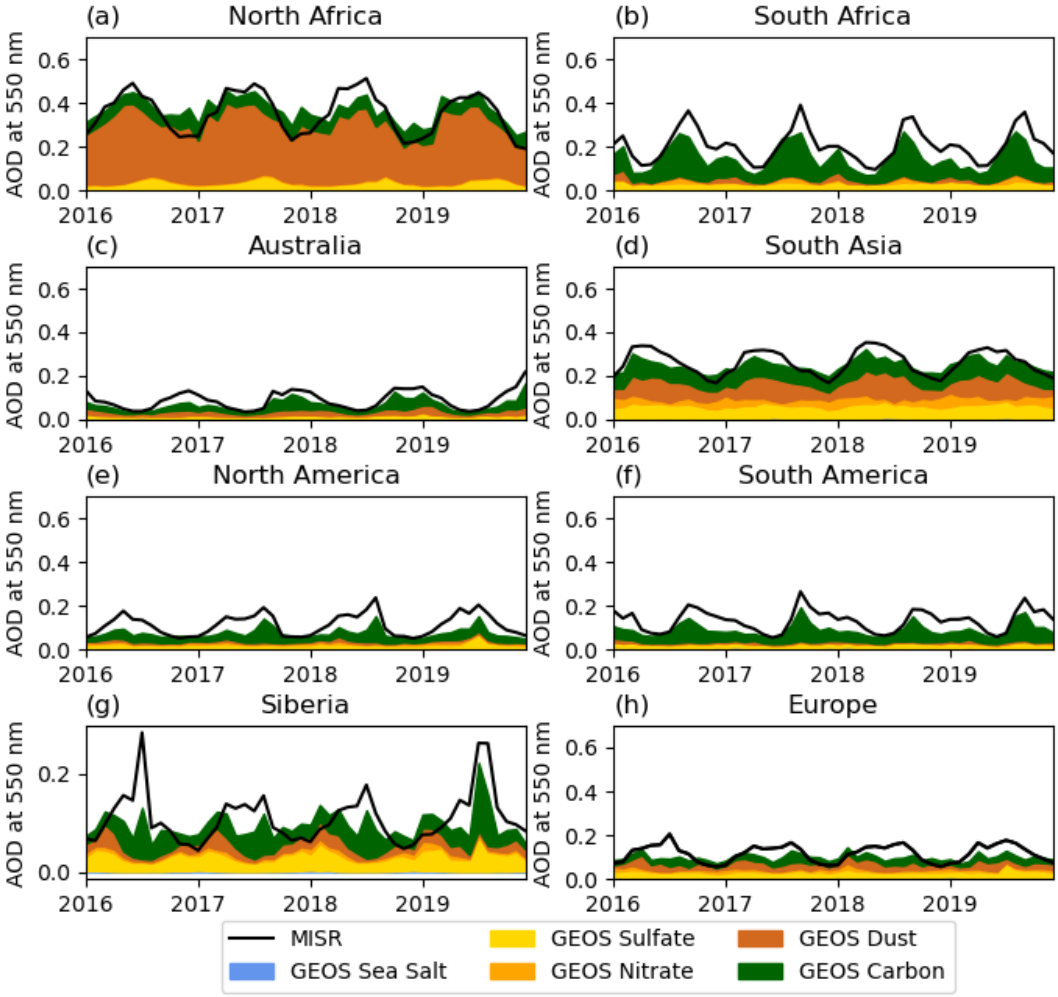

Figure S11: Timeseries of area-averaged monthly mean AOD from MISR and the speciated AOD from the GEOS GOCART2G benchmark simulation over (a) North Africa, (b) South Africa, (c) Australia, (d) South Asia, (e) North America, (f) South America, (g) Siberia, and (h) Europe.

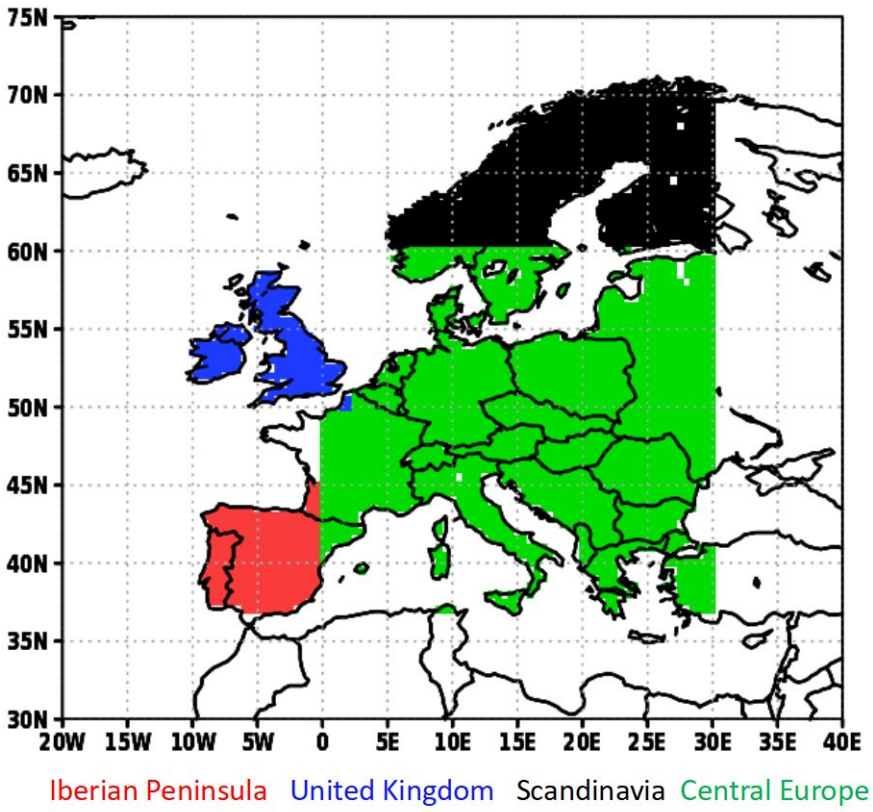

Figure S12: Map of regions used for the area averaged AOD over Europe

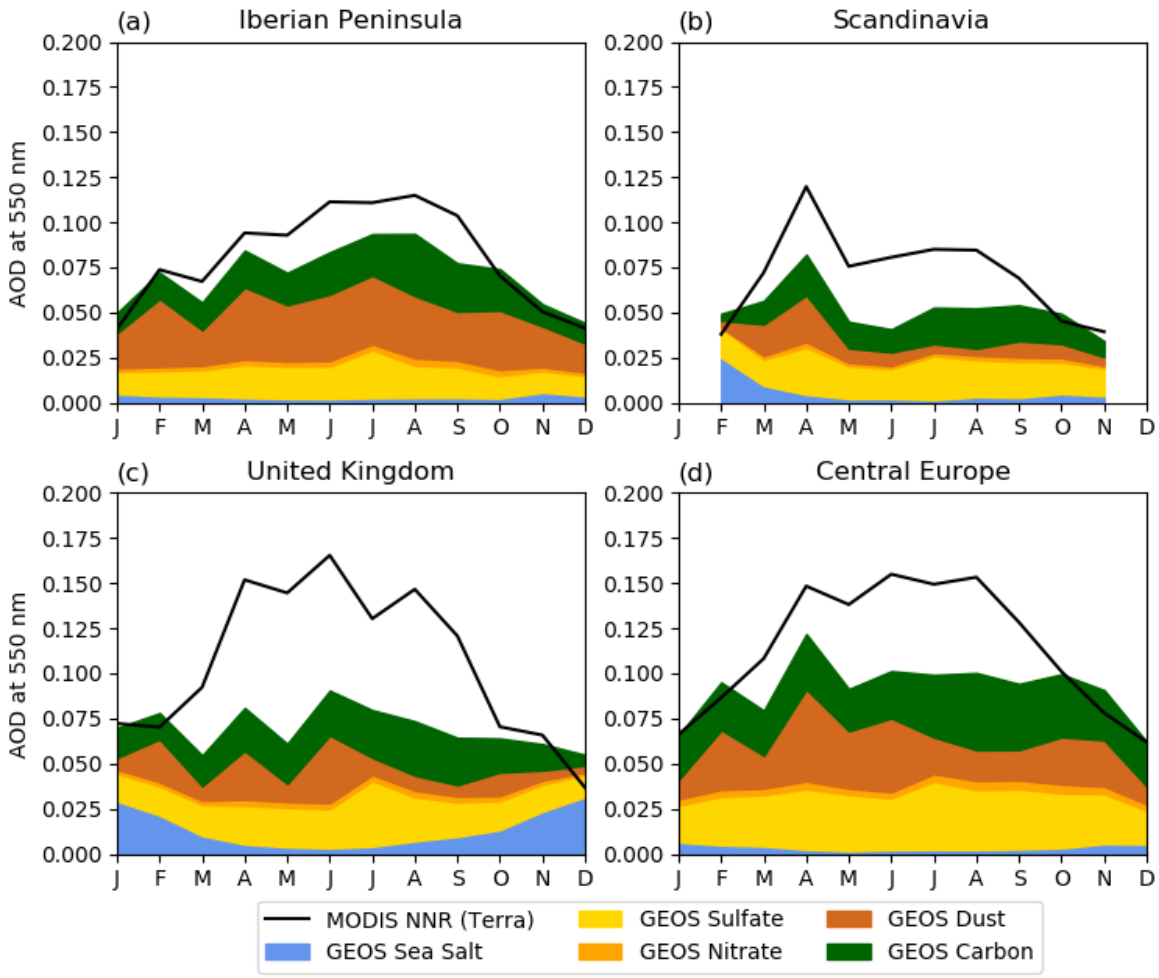

Figure S13: Timeseries of area-averaged monthly mean AOD from the Terra MODIS NNR observational product and the speciated AOD from the GEOS GOCART2G benchmark simulation over (a) the Iberian Peninsula, (b) Scandinavia, (c) the United Kingdom, and (d) central Europe.

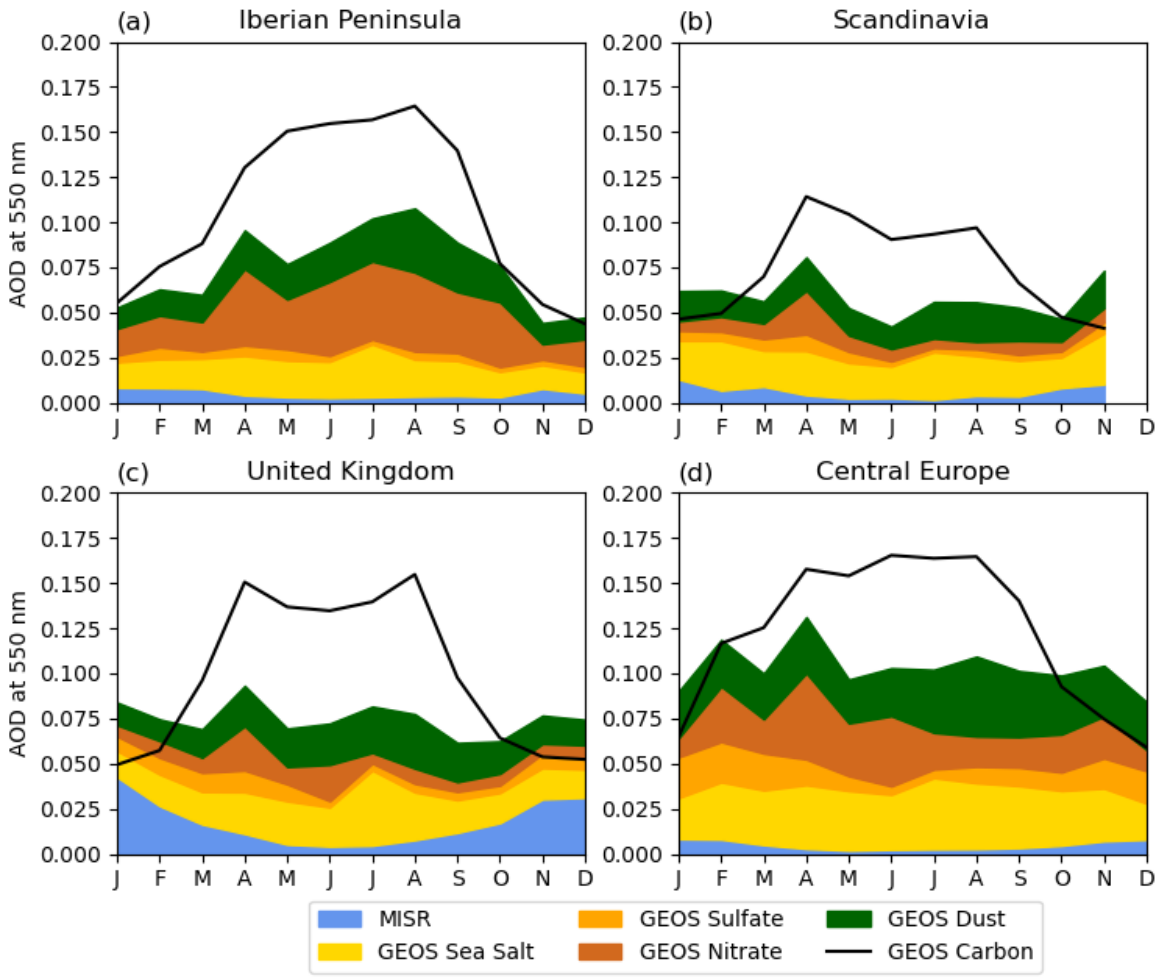

Figure S14: Timeseries of area-averaged monthly mean AOD at 550 nm from the Terra MODIS NNR observational product and the speciated AOD from the GEOS GOCART2G benchmark simulation over (a) the Iberian Peninsula, (b) Scandinavia, (c) the United Kingdom, and (d) central Europe.

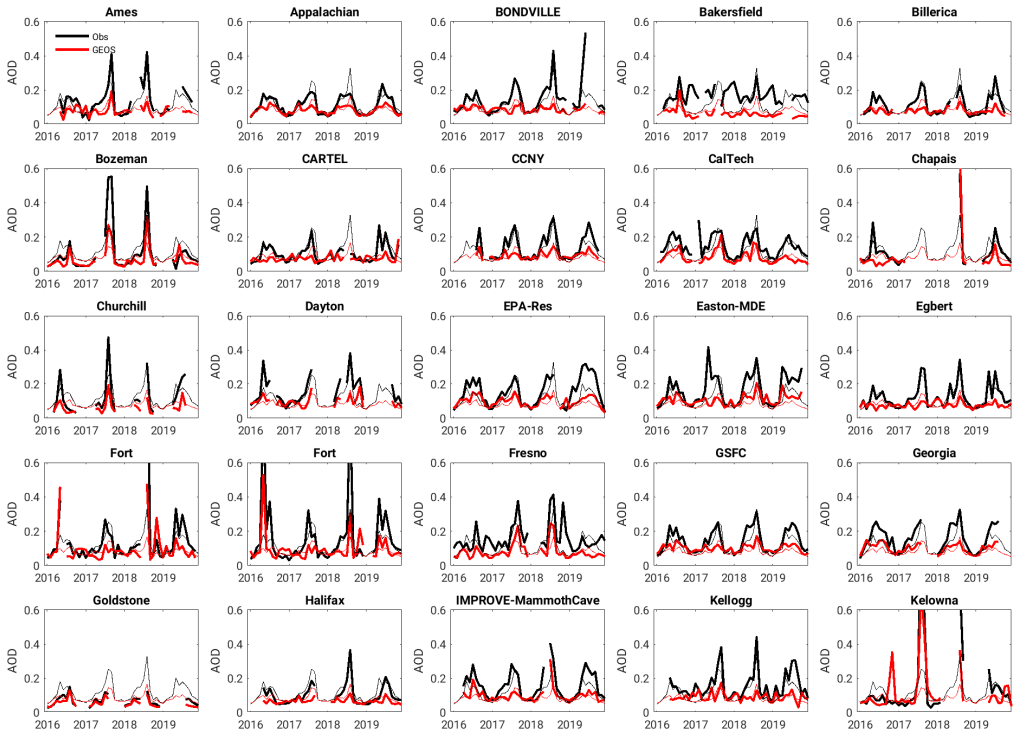
Ames
Appalachian
BONDVILLE
Bakersfield
Billerica
Bozeman
CARTEL
CCNY
CalTech
Chapais
Churchill
Dayton
EPA-Res
Easton-MDE
Egbert
Fort
Fort
Fresno
GSFC
Georgia
Goldstone
Halifax
IMPROVE-MammothCave
Kellogg
Kelowna
Obs
GEOS
AOD
0
0.2
0.4
0.6
2016
2017
2018
2019

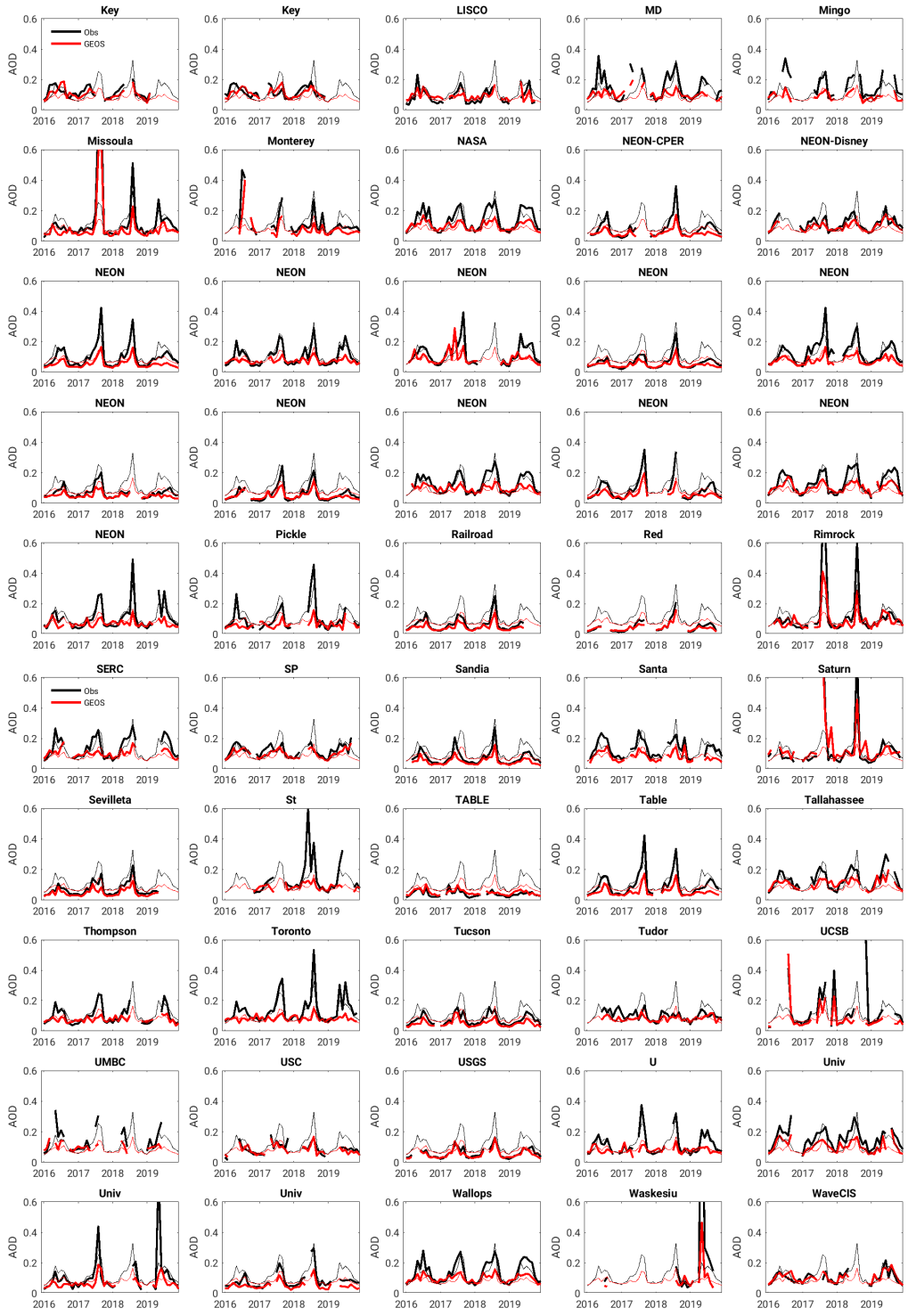

Figure S15: Time series of AOD at 550 nm from GEOS and AERONETsites across the United States and Canada (bold lines). Thin lines indicate the mean for all sites.

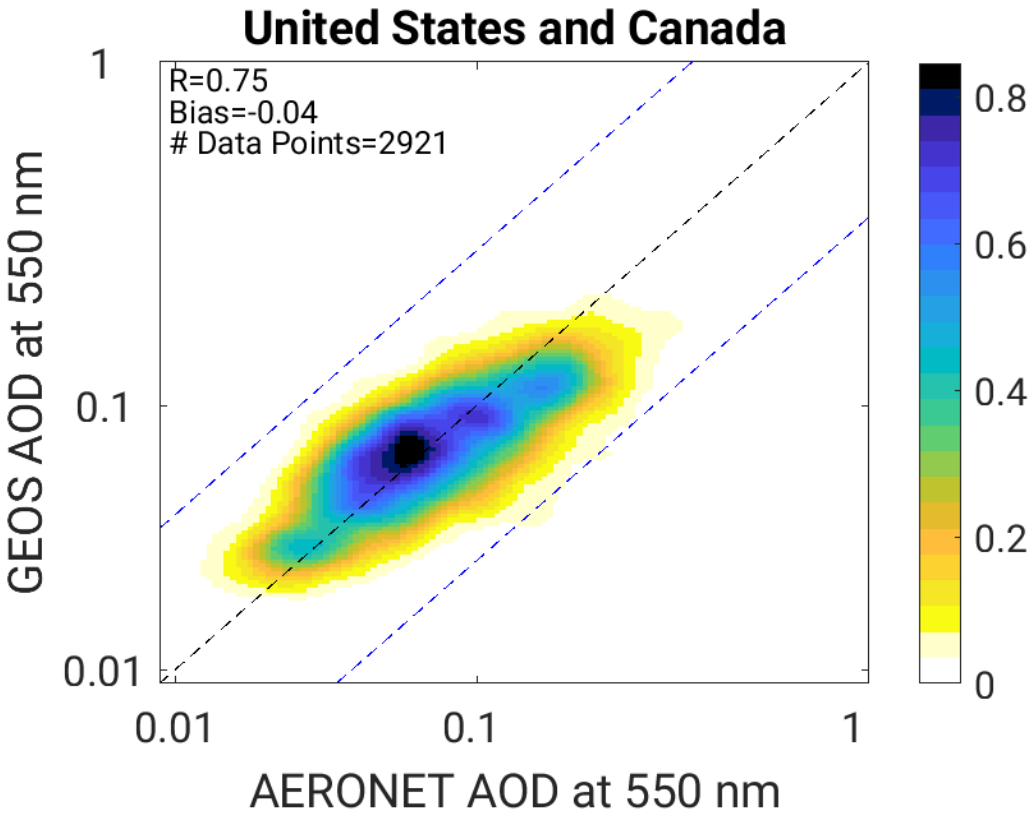

Figure S16: 2-D kernel density estimate for AOD at 550 nm computed as log(AOD+0.01) from 77 AERONET stations across the United States and Canada for co-located data points from the observations and the GOCART-2G benchmark simulation. The statistics are computed as log(AOD+0.01). The black dashed line in (b) and (d) indicates the one-to-one line with the blue dashed lines are the one-to-one line plus or minus one of the one-to-one line.

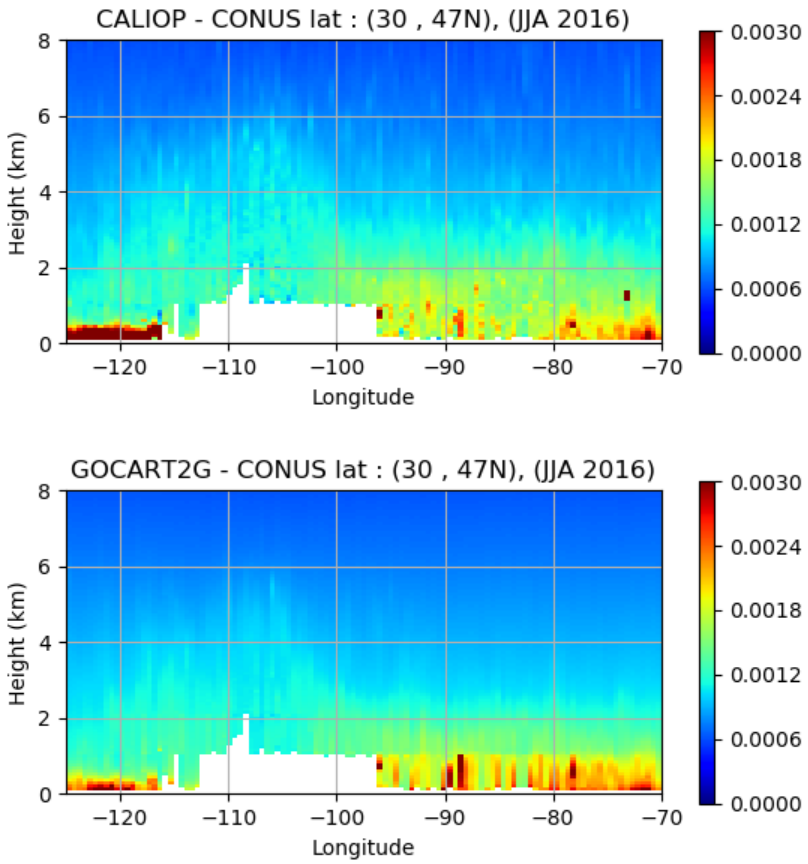

Figure S17: Regional 3-month average (JJA 2016) of CALIOP attenuated backscatter coefficient ($km^{-1}sr^{-1}$) at 532nm over the continental United States (30ºN-47ºN, 120ºW-70ºW) on the top. On the bottom, GEOS GOCART2G attenuated backscatter coefficient sampled on the CALIPSO track for the same period.

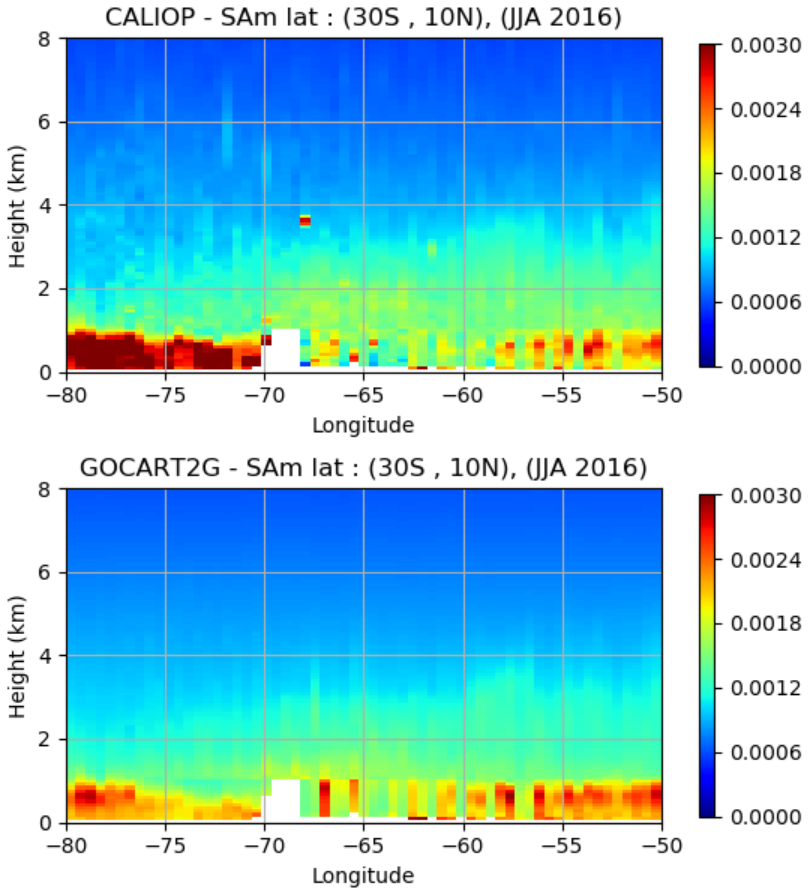

Figure S18: Same as figure S17 but over South America (30ºS-10ºN, 60ºE-20ºE).

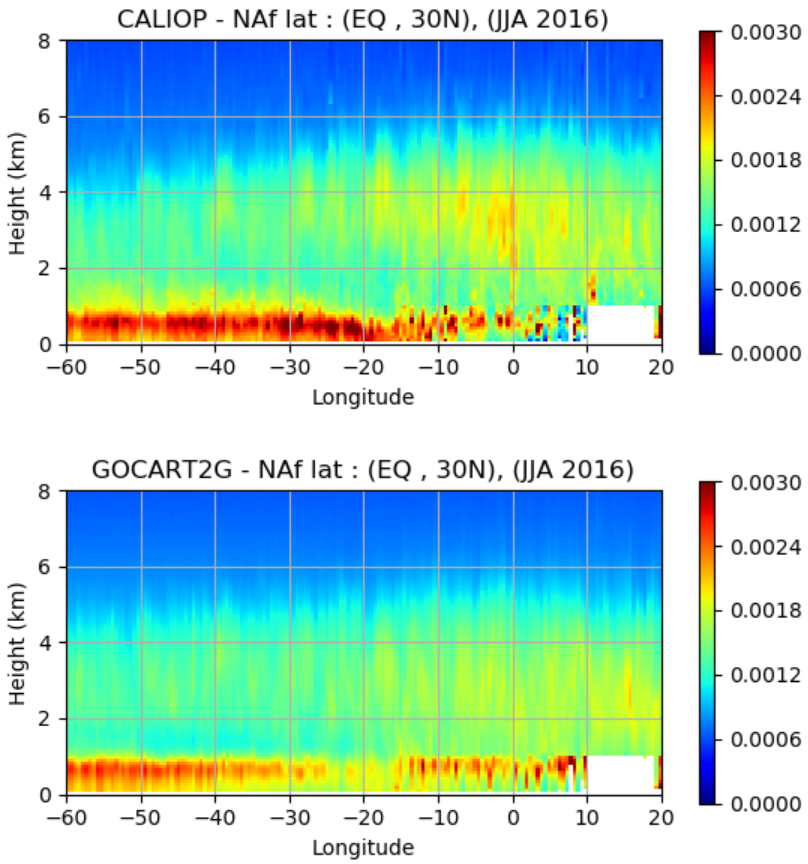

Figure S19: Same as figure S17 but over northern Africa (Eq-30^{o}N, 60^{oE}-20^{o}E).

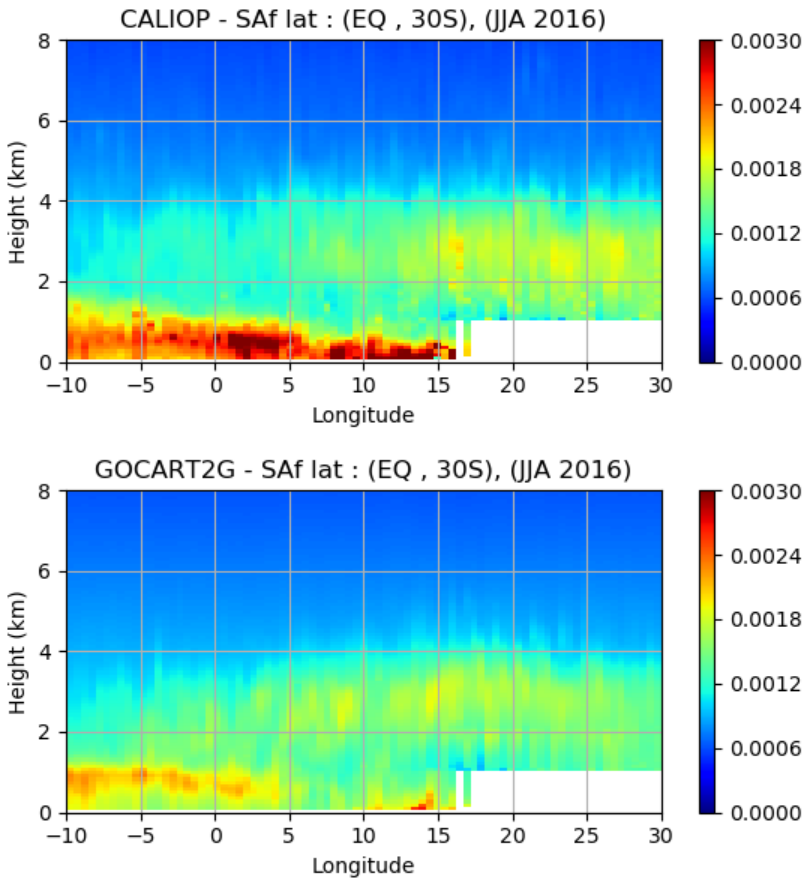

Figure S20: Same as figure S17 but over southern Africa (30°S-Eq, 10°W-30°E).

S3. Required Imports for GOCART-2G

Table S1: Imports required for GOCART-2G

Variable Short Name	Variable Long Name	Dimensions	Component GridComp
DELP	Pressure Thickness	xyz	GOCART2G, Carbon, Dust, Nitrate, Sea Salt, Sulfate
AIRDENS	Air Density	xyz	GOCART2G, Carbon, Dust, Nitrate, Sea Salt, Sulfate
T	Air Temperature	xyz	GOCART2G, Carbon, Dust, Nitrate, Sea Salt, Sulfate
PLE	Air Pressure	xyz	GOCART2G, Carbon, Dust, Nitrate, Sea Salt
FROCEAN	Fraction of Ocean	xy	Carbon, Sea Salt, Sulfate
FRACI	Ice Covered Fraction of Tile	xy	Carbon, Sea Salt

FRLAKE	Fraction of Lake	xy	Carbon, Dust, Sea Salt
LWI	Land-Ocean-Ice Mask	xy	Carbon, Dust, Nitrate, Sea Salt, Sulfate
TROPP	Tropopause Pressure	xy	Carbon, Dust, Nitrate, Sea Salt, Sulfate
U10M	10 m Eastward Wind	xy	Carbon, Dust, Sea Salt, Sulfate
V10M	10 m Northward Wind	xy	Carbon, Dust, Sea Salt, Sulfate
AREA	Grid Cell Area	xy	Carbon, Dust, Nitrate, Sea Salt, Sulfate
ZPBL	Planetary Boundary Layer Height	xy	Carbon, Dust, Nitrate, Sea Salt, Sulfate
SH	Sensible Heat Flux	xy	Carbon, Dust, Nitrate, Sea Salt, Sulfate
Z0H	Surface Roughness for heat	xy	Carbon, Dust, Nitrate, Sea Salt, Sulfate
CN_PRCP	Surface Convective Rain Flux	xy	Carbon, Dust, Nitrate, Sea Salt, Sulfate
NCN_PRCP	Non-convective Precipitation	xy	Carbon, Dust, Nitrate, Sea Salt, Sulfate
RH2	Relative Humidity after Moist	xyz	Carbon, Dust, Nitrate, Sea Salt, Sulfate
ZLE	Geopotential Height	xyz	Carbon, Dust, Nitrate, Sea Salt, Sulfate
PFL_LSAN	3D Flux of liquid non-convective precipitation	xyz	Carbon, Dust, Nitrate, Sea Salt, Sulfate
PFI_LSAN	3D Flux of ice non-convective precipitation	xyz	Carbon, Dust, Nitrate, Sea Salt, Sulfate
U	Eastward Wind	xyz	Carbon, Dust, Nitrate, Sea Salt, Sulfate
V	Northward Wind	xyz	Carbon, Dust, Nitrate, Sea Salt, Sulfate
OC_AIRCRAFT	Aircraft Emissions of Organic Carbon	xyz	Carbon
BC_AIRCRAFT	Aircraft Emissions of Black Carbon	xyz	Carbon
BRC_AIRCRAFT	Aircraft Emissions of Brown Carbon	xyz	Carbon
pSOA_ANTHRO_VOC	SOA from Anthropogenic VOC	xyz	Carbon
pSOA_BIOB_VOC	SOA from Biomass Burning VOC	xyz	Carbon
OC_BIOMASS	Biomass Burning Emissions of OC	xy	Carbon
OC_ISOPRENE	Source Species	xy	Carbon

OC_MTPA	Source Species	xy	Carbon
OC_LIMO	Source Species	xy	Carbon
OC_Biofuel	Biofuel Emissions of OC	Xy	Carbon
OC_ANTEOC1	Anthropogenic Biofuel Emissions	xy	Carbon
OC_ANTEOC2	Anthropogenic Fossil Fuel Emissions	xy	Carbon
OC_SHIP	Ship Emissions of OC	xy	Carbon
OC_Aviation_LTO	Landing/Take-off Aircraft Emissions of OC	xy	Carbon
OC_Aviation_CDS	Climb/Descent Aircraft Emissions of OC	xy	Carbon
OC_Aviation_CRS	Cruise Aircraft Emissions of OC	xy	Carbon
BC_BIOMASS	Biomass Burning Emissions of BC	xy	Carbon
BC_Biofuel	Biofuel Emissions of BC	xy	Carbon
BC_ANTEBC1	Anthropogenic Biofuel Emissions of BC	xy	Carbon
BC_ANTEBC2	Anthropogenic Fossil Fuel Emissions of BC	xy	Carbon
BC_SHIP	Ship Emissions of BC	xy	Carbon
BC_Aviation_LTO	Landing/Take-off Aircraft Emissions of BC	xy	Carbon
BC_Aviation_CDS	Climb/Descent Aircraft Emissions of BC	xy	Carbon
BC_Aviation_CRS	Cruise Aircraft Emissions of BC	xy	Carbon
BRC_Biofuel	Biofuel Emissions of BRC	xy	Carbon
BRC_ANTEOC1	Anthropogenic Biofuel Emissions of BRC	xy	Carbon
BRC_ANTEOC2	Anthropogenic Fossil Fuel Emissions of BRC	xy	Carbon
BRC_SHIP	Ship Emissions of BRC	xy	Carbon
BRC_Aviation_LTO	Landing/Take-off Aircraft Emissions of BRC	xy	Carbon
BRC_Aviation_CDS	Climb/Descent Aircraft Emissions of BRC	xy	Carbon
BRC_Aviation_CRS	Cruise Aircraft Emissions of BRC	xy	Carbon
BRC_TERPENE	Biomass Terpene Emissions	xy	Carbon
DU_SRC	Dust Emission Source	xy	Dust
WET1	Surface Soil Wetness	xy	Dust

USTAR	Surface Velocity Scale	xy	Dust, Nitrate, Sea Salt, Sulfate
EMI_NH3_AG	Agriculture Emissions of NH_3	xy	Nitrate
EMI_NH3_BB	Biomass Burning Emissions of NH_3	xy	Nitrate
EMI_NH3_EN	Energy Emissions of NH_3	xy	Nitrate
EMI_NH3_IN	Industry Emissions of NH_3	xy	Nitrate
EMI_NH3_OC	Ocean Emissions of NH_3	xy	Nitrate
EMI_NH3_RE	Residential Emissions of NH_3	xy	Nitrate
EMI_NH3_TR	Transport Emissions of NH_3	xy	Nitrate
Nitrate_HNO3	Nitrate HNO_3 Emissions	xyz	Nitrate
DU	Dust Mixing Ratio for All Bins	xyz	Nitrate
SS	Sea Salt Mixing Ratio for All Bins	xyz	Nitrate
SU	Sulfate Mixing Ratio	xyz	Nitrate
TS	Surface Skin Temperature	xy	Sea Salt
DZ	Surface Layer Height	xy	Sea Salt
FCLD	Cloud Fraction for Radiation	xyz	Sulfate
pSO2_OCS	Source Species	xyz	Sulfate
SU_AIRCRAFT	Aircraft Emissions	xyz	Sulfate
SU_NO3	Climatological NO3	xyz	Sulfate
SU_OH	Climatological OH	xyz	Sulfate
SU_H2O2	Climatological H_2O_2	xyz	Sulfate
SU_BIOMASS	Biomass Burning Emissions	xy	Sulfate
SU_ANTHROL1	Anthropogenic Biofuel Emissions	xy	Sulfate
SU_ANTHROL2	Anthropogenic Fossil Fuel Emissions	xy	Sulfate
SU_SHIPSO2	SO_2 Shipping Emissions	xy	Sulfate
SU_SHIPSO4	SO_4 Shipping Emissions	xy	Sulfate
SU_DMSO	DMS Emissions	xy	Sulfate
SU_AVIATION_LTO	Landing/Take-off Aircraft Emissions	xy	Sulfate
SU_ AVIATION_CDS	Climb/Descent Aircraft Emissions	xy	Sulfate
SU_ AVIATION_CRS	Cruise Aircraft Emissions	xy	Sulfate

S4. Sample Timings for GEOS

Timers were turned on for a 16-day segment with legacy GOCART and GOCART-2G without StratChem. The chemistry component of the model accounted for 26.44% of the run time with legacy GOCART, of which 22.58% was from GOCART itself. This was reduced to 21.14% is response to the improved code in GOCART-2G, with 16.19% from the aerosol module. However, with the addition of new tracers for brown carbon and secondary organic aerosol, the time to transport the aerosols increased in GOCART-2G. In the segments with the timers on, the model throughput was 76.86 days per day with legacy GOCART and 83.62 days per day with GOCART-2G. Additional details for the timings within each version of GOCART are shown below.

S4.1 GOCART-2G

Times for component <GOCART2G>

	Min			Mean			Max			PE		# cycles
Name	%	inclusive	exclusive	%	inclusive	exclusive	%	inclusive	exclusive	max	min	
GOCART2G	0.00	2398.24	0.02	0.00	2681.19	0.03	0.00	2994.81	0.03	00118	00177	12355
--SetService	0.00	0.08	0.06	0.00	0.14	0.12	0.01	0.18	0.16	00199	00033	1
----generic	0.00	0.02	0.02	0.00	0.02	0.02	0.00	0.03	0.03	00136	00198	1
--Initialize	0.00	12.89	0.02	0.00	12.90	0.03	0.00	12.92	0.04	00006	00108	1
----DU	0.21	5.02	5.02	0.19	5.02	5.02	0.17	5.05	5.05	00139	00097	1
----SS	0.21	4.92	4.92	0.18	4.94	4.94	0.17	4.95	4.95	00033	00139	1
----CA.oc	0.02	0.38	0.38	0.01	0.39	0.39	0.01	0.40	0.40	00087	00203	1
----CA.bc	0.02	0.44	0.44	0.02	0.45	0.45	0.02	0.46	0.46	00215	00027	1
----CA.br	0.02	0.42	0.42	0.02	0.42	0.42	0.02	0.45	0.45	00184	00060	1
----SU	0.03	0.75	0.75	0.03	0.78	0.78	0.03	0.79	0.79	00215	00184	1
----NI	0.03	0.82	0.82	0.03	0.83	0.83	0.03	0.85	0.85	00095	00215	1
----generic	0.00	0.03	0.03	0.00	0.03	0.03	0.00	0.04	0.04	00204	00094	1
--Record	0.00	1.06	0.08	0.00	1.10	0.08	0.00	1.26	0.10	00020	00205	3072
----DU	0.01	0.15	0.15	0.01	0.16	0.16	0.01	0.18	0.18	00180	00002	3072
----SS	0.01	0.15	0.15	0.01	0.16	0.16	0.01	0.17	0.17	00180	00002	3072
----CA.oc	0.00	0.12	0.12	0.00	0.12	0.12	0.00	0.14	0.14	00180	00002	3072
----CA.bc	0.00	0.12	0.12	0.00	0.12	0.12	0.00	0.14	0.14	00100	00002	3072
----CA.br	0.00	0.11	0.11	0.00	0.12	0.12	0.00	0.14	0.14	00180	00115	3072
----SU	0.01	0.16	0.16	0.01	0.16	0.16	0.01	0.19	0.19	00180	00123	3072
----NI	0.01	0.17	0.17	0.01	0.18	0.18	0.01	0.20	0.20	00180	00177	3072
----generic	0.00	0.00	0.00	0.00	0.00	0.00	0.00	0.00	0.00	00180	00137	3072
--Run	0.00	103.81	0.01	0.00	106.46	0.01	0.00	110.28	0.01	00180	00080	4608
----GenRunMine	4.33	103.80	103.80	3.97	106.45	106.45	3.68	110.26	110.26	00180	00204	4608
--Run2	0.00	2269.48	0.01	0.00	2552.25	0.01	0.00	2867.05	0.02	00152	00016	4608
----GenRunMine	94.74	2269.46	2269.46	95.19	2552.23	2552.23	95.56	2867.04	2867.04	00016	00061	4608
--Refresh	0.00	0.39	0.00	0.00	0.42	0.00	0.00	0.45	0.00	00070	00002	64
----GenRefreshTot	0.00	0.39	0.00	0.00	0.42	0.01	0.00	0.45	0.01	00007	00000	64
------DU	0.00	0.05	0.05	0.00	0.06	0.06	0.00	0.07	0.07	00192	00203	64
------SS	0.00	0.05	0.05	0.00	0.06	0.06	0.00	0.07	0.07	00192	00174	64
------CA.oc	0.00	0.04	0.04	0.00	0.05	0.05	0.00	0.05	0.05	00000	00174	64
------CA.bc	0.00	0.04	0.04	0.00	0.04	0.04	0.00	0.05	0.05	00000	00173	64
------CA.br	0.00	0.04	0.04	0.00	0.04	0.04	0.00	0.05	0.05	00000	00137	64
------SU	0.00	0.07	0.07	0.00	0.07	0.07	0.00	0.08	0.08	00140	00173	64
------NI	0.00	0.08	0.08	0.00	0.08	0.08	0.00	0.09	0.09	00180	00009	64
------GenRefreshMine	0.00	0.00	0.00	0.00	0.00	0.00	0.00	0.00	0.00	00020	00043	64
--Finalize	0.00	7.89	0.00	0.00	7.89	0.00	0.00	7.90	0.00	00048	00201	1
----DU	0.09	2.07	2.07	0.08	2.07	2.07	0.07	2.07	2.07	00204	00000	1
----SS	0.09	2.07	2.07	0.08	2.07	2.07	0.07	2.07	2.07	00000	00149	1
----CA.oc	0.02	0.54	0.54	0.02	0.54	0.54	0.02	0.54	0.54	00001	00000	1
----CA.bc	0.02	0.54	0.54	0.02	0.54	0.54	0.02	0.54	0.54	00147	00212	1
----CA.br	0.02	0.55	0.55	0.02	0.55	0.55	0.02	0.56	0.56	00213	00149	1
----SU	0.04	0.96	0.96	0.04	0.96	0.96	0.03	0.96	0.96	00000	00054	1
----NI	0.05	1.16	1.16	0.04	1.17	1.17	0.04	1.17	1.17	00214	00000	1
----generic	0.00	0.00	0.00	0.00	0.00	0.00	0.00	0.00	0.00	00000	00072	1

S4.2 Legacy GOCART

Times for component <GOCART>

Name	Min %	Min inclusive	Min exclusive	Mean %	Mean inclusive	Mean exclusive	Max %	Max inclusive	Max exclusive	PE max	PE min	# cycles
GOCART	0.00	4041.37	0.03	0.00	4079.13	0.03	0.00	4129.80	0.05	00146	00202	12355
--SetService	0.01	0.20	0.20	0.01	0.22	0.22	0.01	0.26	0.26	00188	00124	1
----generic	0.00	0.00	0.00	0.00	0.00	0.00	0.00	0.00	0.00	00026	00010	1
--Initialize	0.00	9.60	0.00	0.00	9.61	0.00	0.00	9.62	0.00	00000	00193	1
----INITIALIZE	0.01	9.60	0.57	0.02	9.61	0.73	0.02	9.62	0.76	00118	00060	1
------generic	0.23	8.86	8.86	0.22	8.88	8.88	0.21	9.05	9.05	00060	00200	1
--Record	0.00	0.98	0.00	0.00	1.02	0.00	0.00	1.09	0.01	00060	00105	3072
----generic	0.02	0.97	0.97	0.02	1.02	1.02	0.03	1.09	1.09	00060	00214	3072
--Run	0.00	161.22	0.01	0.00	163.71	0.01	0.00	166.15	0.02	00157	00180	4608
----GenRunMine	0.00	161.21	0.06	0.00	163.69	0.07	0.00	166.14	0.09	00060	00202	4608
------RUN	0.65	161.14	25.50	0.64	163.63	26.00	0.62	166.07	26.21	00028	00207	4608
--------AERO1	0.00	135.20	0.09	0.00	137.63	0.11	0.00	140.10	0.14	00100	00202	4608
----------DU	0.02	0.92	0.92	0.03	1.06	1.06	0.03	1.42	1.42	00029	00214	4608
----------SS	0.20	7.88	7.88	0.19	7.94	7.94	0.19	8.05	8.05	00175	00174	4608
----------BC	1.20	47.00	47.00	1.20	48.91	48.91	1.22	51.80	51.80	00207	00000	4608
----------OC	1.58	61.66	61.66	1.51	61.68	61.68	1.46	61.68	61.68	00203	00012	4608
----------SU	0.41	16.12	16.12	0.42	17.00	17.00	0.46	19.32	19.32	00089	00213	4608
----------NI	0.02	0.87	0.87	0.02	0.94	0.94	0.03	1.22	1.22	00054	00200	4608
--Run2	0.00	3859.26	0.01	0.00	3897.76	0.01	0.00	3947.32	0.02	00157	00163	4608
----GenRunMine	0.00	3859.24	0.08	0.00	3897.75	0.09	0.00	3947.31	0.11	00054	00204	4608
------RUN	0.73	3859.15	28.53	0.72	3897.65	29.48	0.74	3947.23	31.42	00077	00215	4608
--------AERO2	0.01	3827.73	0.22	0.01	3868.17	0.27	0.01	3918.23	0.33	00140	00202	4608
----------CO	1.95	76.08	76.08	2.11	86.03	86.03	2.11	89.47	89.47	00034	00207	4608
----------CO2	0.05	1.98	1.98	0.06	2.32	2.32	0.06	2.70	2.70	00063	00129	4608
----------DU	14.66	572.93	572.93	14.91	608.15	608.15	14.88	630.09	630.09	00209	00077	4608
----------SS	18.38	718.27	718.27	17.93	731.56	731.56	17.61	745.95	745.95	00141	00145	4608
----------BC	5.28	206.57	206.57	5.69	232.11	232.11	6.04	255.71	255.71	00002	00141	4608
----------OC	5.26	205.45	205.45	5.40	220.37	220.37	5.66	239.94	239.94	00040	00002	4608
----------SU	6.99	273.05	273.05	7.21	293.97	293.97	7.14	302.39	302.39	00032	00040	4608
----------CFC	2.35	91.68	91.68	2.76	112.52	112.52	3.08	130.55	130.55	00092	00201	4608
----------NI	39.82	1556.26	1556.26	38.76	1580.87	1580.87	38.22	1618.81	1618.81	00173	00092	4608
--Refresh	0.00	0.72	0.00	0.00	0.77	0.00	0.00	0.86	0.00	00017	00131	64
----GenRefreshTot	0.00	0.72	0.00	0.00	0.77	0.00	0.00	0.86	0.00	00177	00002	64
------GenRefreshMine	0.02	0.72	0.72	0.02	0.77	0.77	0.02	0.86	0.86	00060	00202	64
--Finalize	0.00	6.01	0.00	0.00	6.01	0.00	0.00	6.01	0.00	00159	00005	1
----FINALIZE	0.00	0.00	0.00	0.00	0.00	0.00	0.00	0.00	0.00	00080	00032	1
----generic	0.15	6.01	6.01	0.15	6.01	6.01	0.14	6.01	6.01	00208	00025	1

S5. References

English, J. M., Toon, O. B., Mills, M. J., and Yu, F.: Microphysical simulations of new particle formation in the upper troposphere and lower stratosphere, Atmos. Chem. Phys., 11, 9303–9322, https://doi.org/10.5194/acp-11-9303-2011, 2011.

Guenther, A. B., Jiang, X., Heald, C. L., Sakulyanontvittaya, T., Duhl, T., Emmons, L. K., and Wang, X.: The Model of Emissions of Gases and Aerosols from Nature version 2.1 (MEGAN2.1): an extended and updated framework for modeling biogenic emissions, Geosci. Model Dev., 5, 1471–1492, https://doi.org/10.5194/gmd-5-1471-2012, 2012.

Hodzic, A. and Jimenez, J. L.: Modeling anthropogenically controlled secondary organic aerosols in a megacity: a simplified framework for global and climate models, Geosci. Model Dev., 4, 901–917, https://doi.org/10.5194/gmd-4-901-2011, 2011.

Keller, C. A., Long, M. S., Yantosca, R. M., Da Silva, A. M., Pawson, S., and Jacob, D. J.: HEMCO v1.0: a versatile, ESMF-compliant component for calculating emissions in atmospheric models, Geosci. Model Dev., 7, 1409–1417, https://doi.org/10.5194/gmd-7-1409-2014, 2014.

Kim, P. S., Jacob, D. J., Fisher, J. A., Travis, K., Yu, K., Zhu, L., Yantosca, R. M., Sulprizio, M. P., Jimenez, J. L., Campuzano-Jost, P., Froyd, K. D., Liao, J., Hair, J. W., Fenn, M. A., Butler, C. F., Wagner, N. L., Gordon, T. D., Welti, A., Wennberg, P. O., Crounse, J. D., Clair, J. M. S., Teng, A. P., Millet, D. B., Schwarz, J. P., Markovic, M. Z., and Perring, A. E.: Sources, seasonality, and trends of southeast US aerosol: an integrated analysis of surface, aircraft, and

satellite observations with the GEOS-Chem chemical transport model, Atmos Chem Phys, 15, 10411 10433, https://doi.org/10.5194/acp-15-10411-2015, 2015.

Nielsen, J., Pawson, S., Molod, A., Auer, B., da Silva, A., Douglass, A., Duncan, B., Liang, Q., Manyin, M., Oman, L., Putman, W., Strahan, S., and Wargan, K.: Chemical Mechanisms and Their Applications in the Goddard Earth Observing System (GEOS) Earth System Model, J. Adv. Model. Earth Syst., 9, 3019–3044, https://doi.org/10.1002/2017MS001011, 2017.

Sander, S. P., J. Abbatt, J. R. Barker, J. B. Burkholder, R. R. Friedl, D. M. Golden, R. E. Huie, C. E. Kolb, M. J. Kurylo, G. K. Moortgat, V. L. Orkin and P. H. Wine "Chemical Kinetics and Photochemical Data for Use in Atmospheric Studies, Evaluation No. 17," JPL Publication 10-6, Jet Propulsion Laboratory, Pasadena, 2011 http://jpldataeval.jpl.nasa.gov.